Erciyes Üniversitesi
Fen Bilimleri Enstitüsü Dergisi
Cilt 40, Sayı 3 , 2024

Erciyes University
Journal of Institue Of Science and Technology
Volume 40, Issue 3, 2024

Manual and Remote-Controlled Secondary Emission Calorimeter Modules for High-Radiation Environments

Nejdet Paran[1,*], Saleh Abubakar[1], Burak Tekgün[2], Emrah Tıraş[1,3,*]

[1] Department of Physics, Faculty of Science, Erciyes University, Kayseri 38030, Türkiye
[2] Department of Electrical Electronics Engineering, School of Engineering, Abdullah Gul University, Kayseri, 38080, Türkiye
[3] Department of Physics and Astronomy, University of Iowa, IA 52242, USA

(Alınış / Received: 10.10.2024, Kabul / Accepted: 19.12.2024, Online Yayınlanma / Published Online: 30.12.2024)

Keywords
Secondary Emission Ionization Calorimetry, Cosmic Radiation, Radiation Detectors, Particle Detectors, PMTs.

Abstract: There is a growing demand for durable and radiation-resistant particle detectors and ionization calorimeters. This demand arises from the increased luminosity and extreme radiation conditions at particle colliders and accelerators. Secondary Emission (SE) Ionization Calorimetry is an innovative technology developed to quantify the energy of electromagnetic and hadronic particles, especially under high-radiation conditions. This study examines the development and radiation testing of the innovative SE modules. The modules were produced by altering the standard Hamamatsu single anode R7761 Photomultiplier Tubes (PMTs). A SPICE model was constructed based on the parameters of the PMT system. The model's objective is to evaluate various divider circuits. Three distinct voltage conditions for the identical modules were established, and the new modules were evaluated utilizing cosmic background and gamma radiation sources. Results indicate that all three modes exhibit significant cosmic and gamma radiation sensitivity. Mode 1 and Mode 2 exhibit substantial signal sizes compared to Mode 3, which results from cosmic particle interactions. The obtained signal sizes are ~70 mV for Mode 1, ~65 mV for Mode 2, and ~8 mV for Mode 3. This study indicates that the SE module is a promising technology for future radiation-resistant nuclear and high-energy detectors. Since such detector systems are either in a high-radiation area or a closed room/box, remote mode changes allow us to continue the experimental process without interruption. We can instantaneously observe the modes' effects by adding these signals to the interface where the modes are controlled.

Yüksek Radyasyonlu Ortamlar için Manuel ve Uzaktan Kumandalı İkincil Emisyon Kalorimetre Modülleri

Anahtar Kelimeler
İkincil Emisyon İyonizasyon Kalorimetrisi, Kozmik Radyasyon, Radyasyon Dedektörleri, Parçacık Dedektörleri, PMT'ler

Öz: Parçacık çarpıştırıcıları ve hızlandırıcılarındaki artan parlaklık ve aşırı radyasyon koşulları nedeniyle, hassas, dayanıklı ve güvenilir, radyasyona dayanıklı parçacık dedektörleri ve iyonizasyon kalorimetrelerine olan talep artmaktadır. İkincil Emisyon (SE) İyonizasyon Kalorimetrisi, özellikle yüksek radyasyon koşulları altında elektromanyetik ve hadronik parçacıkların enerjisini ölçmek için geliştirilmiş yenilikçi bir teknolojidir. Bu çalışma, yeni SE modüllerinin geliştirilmesini ve radyasyon testlerini incelemektedir. Modüller, standart Hamamatsu tek anotlu R7761 Fotoçoğaltıcı Tüpler (PMT'ler) değiştirilerek üretilmiştir. PMT sisteminin parametrelerine dayalı bir SPICE modeli oluşturulmuştur. Modelin amacı çeşitli bölücü devrelerle incelemektir. Aynı modül için üç farklı voltaj koşulu oluşturulmuş ve yeni modüller kozmik arka plan ve gama radyasyon kaynakları kullanılarak ölçümler alınmıştır. Sonuçlar, her üç modun da

önemli ölçüde kozmik ve gama radyasyon hassasiyeti sergilediğini göstermektedir. Mod 1 ve Mod 2, kozmik parçacık etkileşimlerinden kaynaklanan sinyal boyutları açısından Mod 3'e kıyasla önemli bir fark sergilemektedir. Elde edilen sinyal boyutları Mod 1 için ~70 mV, Mod 2 için ~65 mV ve Mod 3 için ~8 mV'dir. Bu çalışma, SE modülünün gelecekteki radyasyona dayanıklı nükleer ve yüksek enerjili dedektörler için potansiyel bir teknoloji olduğunu göstermektedir. Bu tür dedektör sistemleri ya yüksek radyasyonlu bir alanda ya da kapalı bir odada/kutuda olduğundan, uzaktan mod değişiklikleri deneysel süreci kesintiye uğratmadan devam ettirmemizi sağlar. Bu sinyalleri modların kontrol edildiği arayüze ekleyerek modların etkilerini anlık olarak gözlemleyebiliriz.

1. Introduction

Energy measurement using calorimetry is one of the widely used techniques in high-energy and nuclear physics to determine the momentum and energies of particles. The principle behind calorimeters is to use crystal, quartz, or plastic scintillators to convert particle showers created by primary particles into light and then use a photodetector to turn that light into electric signals. Calibration and long-term signal efficiency are critical issues for plastic scintillators and crystalline material calorimeters operating in strong radiation conditions. Quartz-based calorimeters are more radiation-resistant and produce fast, narrow-band signals. However, they have a lower signal output and primarily detect the electromagnetic core of hadronic showers. In contrast, calorimeters made of crystalline materials or plastic scintillators struggle with long-term signal efficiency and calibration in high-radiation environments [1–7].

To overcome these obstacles, active research programs in the field are concentrating on enhancing light yield, radiation resistance, and active materials. In situations with high-radiation levels, a unique method for measuring electromagnetic shower particles is the Secondary Emission Ionization (SE) calorimetry [8–16]. Developing SE calorimeters is one of the main focuses of the research and development groups in the field of High Energy and Accelerator Physics. Apart from the commonly employed techniques for calorimeter performance development and enhancement, we devised a unique method that alters the voltage applied just to the photocathode and first dynode while maintaining the basic structure of photomultiplier tubes (PMTs). This research aims to design and fabricate a remotely controllable baseboard for SE calorimetry and related calorimetric uses and evaluate the newly developed module using gamma and cosmic sources. This study alters and redesigns the conventional PMT bias circuit to deal with numerous anode signal outputs to characterize various operation modes. The design of various operational modes and the characterization measurements of both secondary emission modes and the conventional PMT mode are examined comprehensively. The required sensor front-end and back-end circuits are designed to enable the different operating modes, which allow fault-tolerant operation of SE calorimetry in radiation-harsh environments.

This paper presents a novel design for remote-controllable SE calorimetry. This design permits dynamic voltage adjustments solely for the photocathode and initial dynode while maintaining the fundamental architecture of the PMTs. This pioneering method is unprecedented in the literature, overcoming the constraints of manual voltage regulation and improving operational adaptability. Additionally, we develop a remote-control circuit integrated with computer interface software to facilitate a smooth transition between various working modes, thereby streamlining the operation of intricate detecting systems. The modules underwent testing with cosmic and gamma radiation in Mode 1, the usual operational mode of photomultiplier tubes (PMTs). The signal dimensions of the PMT were measured at voltages marginally below (1800V) and above (2200V) the typical working voltage of 2000V. This flexibility to various working modes guarantees the system's versatility and robustness, instilling confidence in readers regarding its prospective uses.

2. Material and Methods

Manual Control

Photomultipliers are very susceptible vacuum tubes that transform light into a quantitative electric current. PMTs transform the inferior light output of the scintillation signal into an observable electrical pulse; scintillators could widely be used in radiation detection and spectroscopy [17]. In this study, we used the Hamamatsu single anode R7761 PMT, previously used to collect data in the CDF experiment at Fermi National Accelerator Laboratory (Fermilab) [18]. R7761 PMT has 19 dynode stages serving as secondary emissive electrodes in a fine mesh structure, and it has a length of 50 mm and a diameter of 39 mm with an operational window diameter of 27 mm [19].

Operation of the R7761 photomultiplier tube requires a voltage source of at least -1700 V and a voltage divider circuit to appropriately allocate this voltage to the PMT's dynodes. In order to get high efficiency from the PMT, providing the appropriate voltage to the dynodes is mandatory. Since supplying each dynode with a separate voltage source is not economical or feasible, a voltage divider circuit is necessary. Therefore, a voltage divider circuit is usually used to supply the appropriate voltage to each dynode of the PMT and a high-voltage power supply is used to feed this circuit. A stable voltage from the high-voltage source is crucial for the proper operation of the PMT. Due to the high number of PMT dynodes, such as R7761, capacitors are added to these dynodes to prevent the voltage drop between the dynodes near the anode. We added a 22nF decoupling capacitor to the last five dynodes of the voltage divider board we designed. Figure 1 shows the schematic diagram of the SE voltage divider for R7761. The circuit schematic shows the baseboards that power and read data from a single PMT in the SE module.

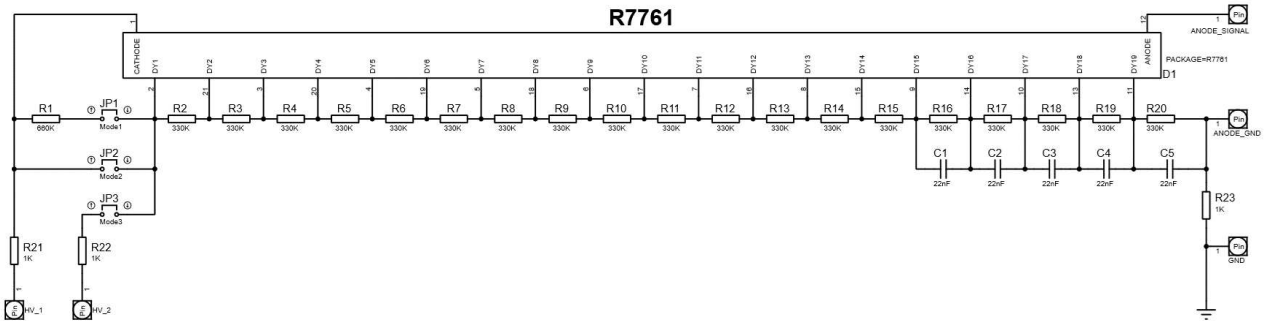

Figure 1. Schematic diagram of the secondary emission voltage divider for R7761 PMTs.

There are three different modes of operation for the baseboards of R7761 single-anode PMTs. High voltage was applied to Mode 1 and Mode 2 via HV1 and to Mode 3 via HV2. An oscilloscope was used for data collection.

Mode 1: JP1 switch is closed. As shown in Figure 2a, the voltage divider chain is unchanged, and the potential difference across the dynodes is equal, except for the two times potential across the Cathode-Dy1 gap. This mode is also the normal operating mode of the Hamamatsu R7761 PMT.

Mode 2: In this mode, the JP2 switch is closed. As shown in Figure 2b, the bridging of the R1 resistor is enabled, and the potential across the Cathode-Dy1 gap is 0 volt.

Mode 3: By closing the JP3 switch, the cathode is isolated from the rest of the divider chain. As shown in Figure 2c, a second voltage input to the baseboard allows for the voltage on Dy1. In this mode, the photocathode may still charge if there is no second high-voltage source.

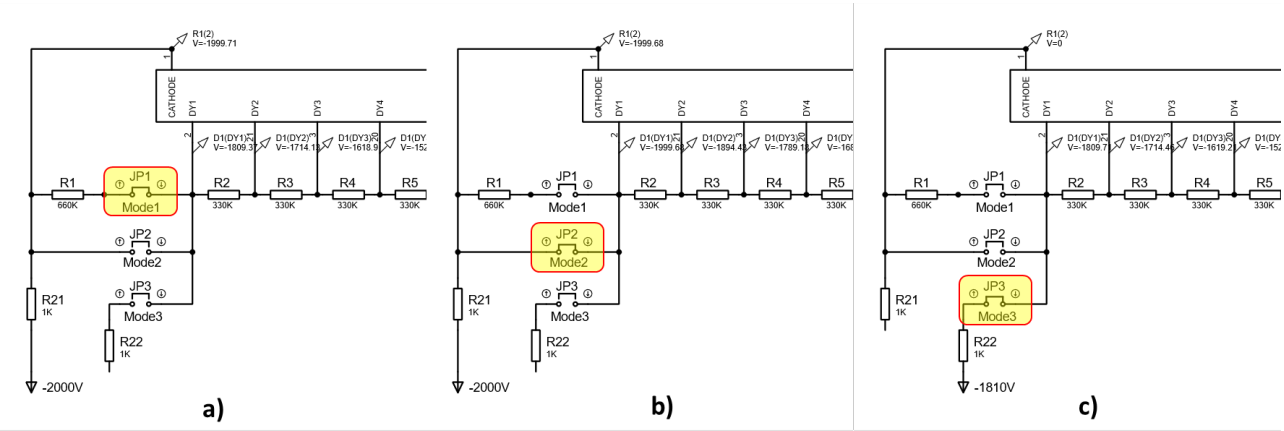

Figure 2. a) Schematic diagram of the secondary emission voltage divider for R7761 PMTs for Mode 1. b) Schematic diagram of the secondary emission voltage divider for R7761 PMTs for Mode 2. c) Schematic diagram of the secondary emission voltage divider for R7761 PMTs for Mode 3

A PCB layout of the manually controlled R7761 PMT is shown in Figures 3a and 3b. Figure 3c shows the printed circuit board with all the soldering and assembly processes done. Two high-voltage inputs were provided with SHV connectors, while BNC connectors were used for the signal. As can be seen in Figure 3c, the photomultiplier detector was wrapped with a light-impermeable foil and then taped with insulating tape to protect it from light.

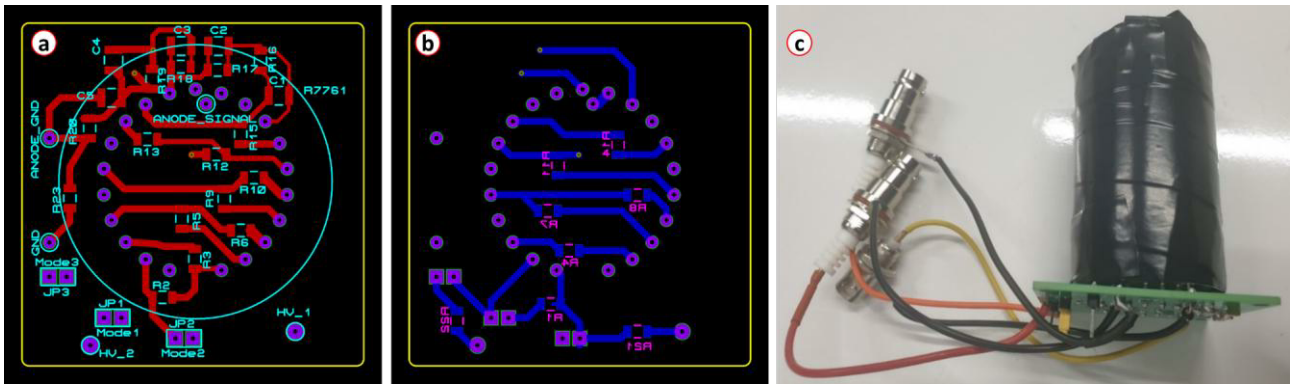

Figure 3. a) PCB layout view of the top side and b) bottom side c) Image of the electronic board with all soldering and assembly processes completed for the manually controlled R7761 type PMT.

Since photomultiplier tubes have a very high sensitivity, they must be protected from light sources other than the radiation to be measured. Otherwise, high noise is generated, and signal acquisition becomes impossible. Using a sheath to protect it from magnetic fields prevents noise in the PMT.

Remote Control

Complex calorimetric systems need to be automatically controlled and managed remotely to be able to run well in high-radiation environments. In addition to increasing operational flexibility, remotely adjustable solutions lessen the need for manual intervention in difficult situations. To meet these demands, we created a remote-control module that enables smooth changes to the PMT operating modes via a computer interface.

Figure 4 shows the schematic diagram of the SE voltage divider circuit for the remote-controlled R7761 photomultiplier tube. This circuit schematic shows the baseboards that power and read data from a single photomultiplier tube. Understanding the high-voltage application points in the voltage divider circuit that drives the PMT is crucial. The only change for the different modes is the points at which the high voltage is applied to the circuit. So, three different high-voltage application points exist for the three modes. In the first mode, the high voltage is applied to the photocathode through a 1kohm resistor and to the first dynode through a 660kohm resistor. In the second mode, the high voltage is applied directly to the photocathode and the first dynode through a 1kohm resistor. Finally, in the third mode, the photocathode was utterly disabled, and the high voltage was applied directly to the first dynode through a 1kohm resistor. In all three modes, the applied voltage value gradually decreases after the first dynode point in the voltage divider circuit since the resistances are equal until it is divided equally and reaches 0V at the anode.

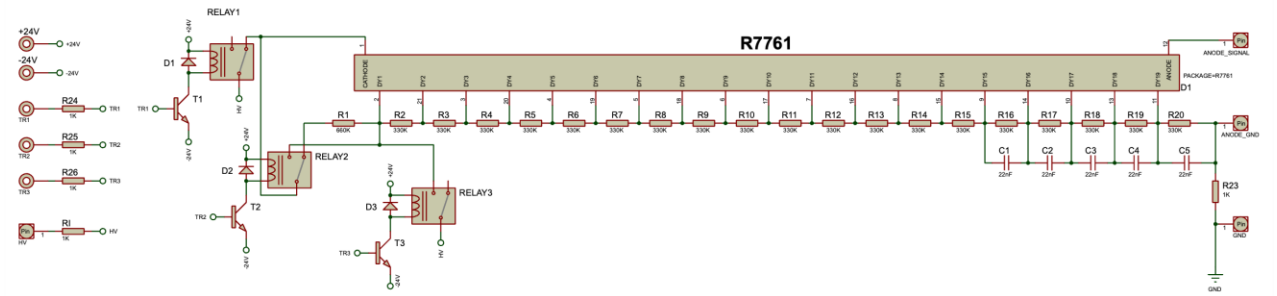

Figure 4. Schematic diagram of the SE voltage divider circuit for the remote-controlled R7761 photomultiplier tube.

The selection of relays for the high-voltage control circuit was not arbitrary. We meticulously chose them to ensure the circuit's performance. Relays were chosen for their affordability, accessibility, ease of control, and reliability as electronic circuit elements. Since the DC coil that switches these relays on and off operates with a nominal voltage of 24V, these relays cannot be directly controlled with the Arduino, which can output 5V. One solution to this problem is to use suitable transistors between the Arduino and the relays. The schematic connections of the relays and transistors are given in Figure 4. The suitable transistor was chosen based on our relay's nominal voltage and coil resistance. This means we must supply the external electronic circuit board with 24VDC to operate the relays. The 24V entering the DC coil of the relay will be connected to the collector of the transistor at the other end of the coil and reach the ground via the emitter. Therefore, the Collector-Emitter Voltage of the transistor must be more than 24V, and the Collector Current (continuous) must be more than 22.5 mA. For the 2N3904 npn transistor we use, the Collector-Emitter Voltage value is 40V, and the Collector Current (continuous) value is 200mA, so it easily meets the desired values.

As mentioned above, since it is impossible to drive a relay with a 24V operating voltage directly with Arduino, it is necessary to put a suitable transistor in between. Depending on the value of the current in the Base leg of the transistor, the amount of current in the Collector leg changes. One factor that determines the value of the current in the Base leg is the value of the resistor connected to the Base leg. In our thorough simulation studies, we can obtain the desired values when we connect a 1k ohm resistor to the Base leg. This emphasis on thorough simulation studies reassures the reader about the circuit's functionality.

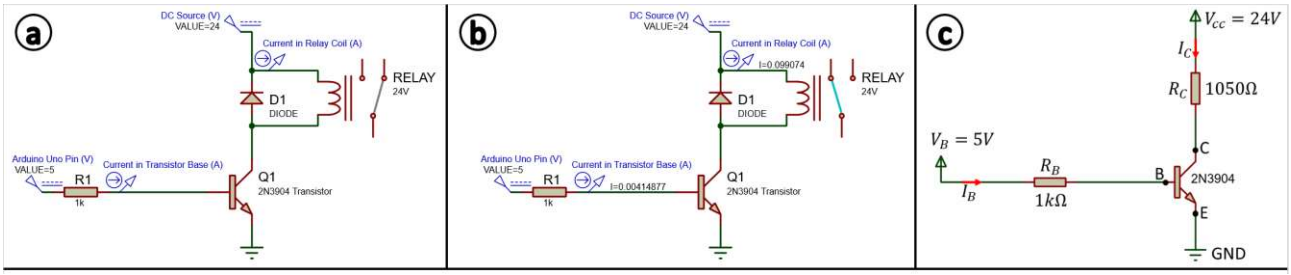

Figure 5. Relay and transistor simulation results are a) when switching OFF, b) when switching ON, and c) equivalent circuits are drawn to solve the current values IC and IB in the relay and transistor circuit diagram using an analytical method.

To compare the simulation result with the analytical solution, let us analyze the circuit using the schematic in Figure 5c. From V_{CC} through C and E to GND, the equation becomes:

$$V_{CC} - I_C \times R_C = 0.$$

If we substitute their values:

$$24V - I_C \times 1k\Omega = 0$$

is found. If we subtract I_C from here, $I_C = 24mA$ is found. This value is close to the 22.8 mA value obtained as a result of simulation.

For the current starting at 5V and ending at GND via B and E, the equation becomes:

$$5V - I_B \times R_B - V_{BE} = 0.$$

If the values are substituted,

$$5V - I_B \times 1k\Omega - 0.7V = 0$$

is found. If we subtract I_B from this equation, then $I_B = 4.3mA$ is found. It is seen that this value is close to the $4.2mA$ value obtained as a result of simulation.

A potential problem in this design was also addressed: When the voltage applied to the relay is switched off, the field induced on the DC winding may cause reverse currents and cause the transistors to fail after a while. This problem was solved by connecting a diode in parallel to the two legs of the DC winding. The diode allows the current to flow in only one direction, preventing the reverse currents that could damage the transistors.

The on/off combinations of transistors by mode, as presented in Table 1, were not randomly chosen. This strategic design, which was based on the operational requirements of each mode, can be created in different ways. Our electronic board design was created according to the combination in Table 1. According to this design, all transistors must be in the LOW (deactivated—not energized) position for the first mode to be active. This choice was a preferential choice. Because the first mode is the basic mode, it eliminates the need to control the electronic board to operate in this mode actively. The second and third modes require active control of the circuit. For the second mode to be active, the first and third transistors must be LOW, and the second transistor must be HIGH (activated-energized). Finally, the first and third transistors must be high for the third mode to be active. In this mode, whether the second transistor is LOW or HIGH does not change the circuit.

Table 1. Transistors combination for modes.

	MODE 1	MODE 2	MODE 3
TRANSISTOR 1	LOW	LOW	HIGH
TRANSISTOR 2	LOW	HIGH	LOW/HIGH
TRANSISTOR 3	LOW	LOW	HIGH

A PCB layout of the remote-controlled R7761 photomultiplier tube is shown in Figures 6a and 6b. Figure 6c shows the printed circuit board with all the soldering and assembly processes done. A high-voltage input is provided with SHV connectors, while a BNC connector is used for the signal. As can be seen in Figure 6c, the photomultiplier detector was wrapped with a light-impermeable foil and then taped with insulating tape to protect it from light.

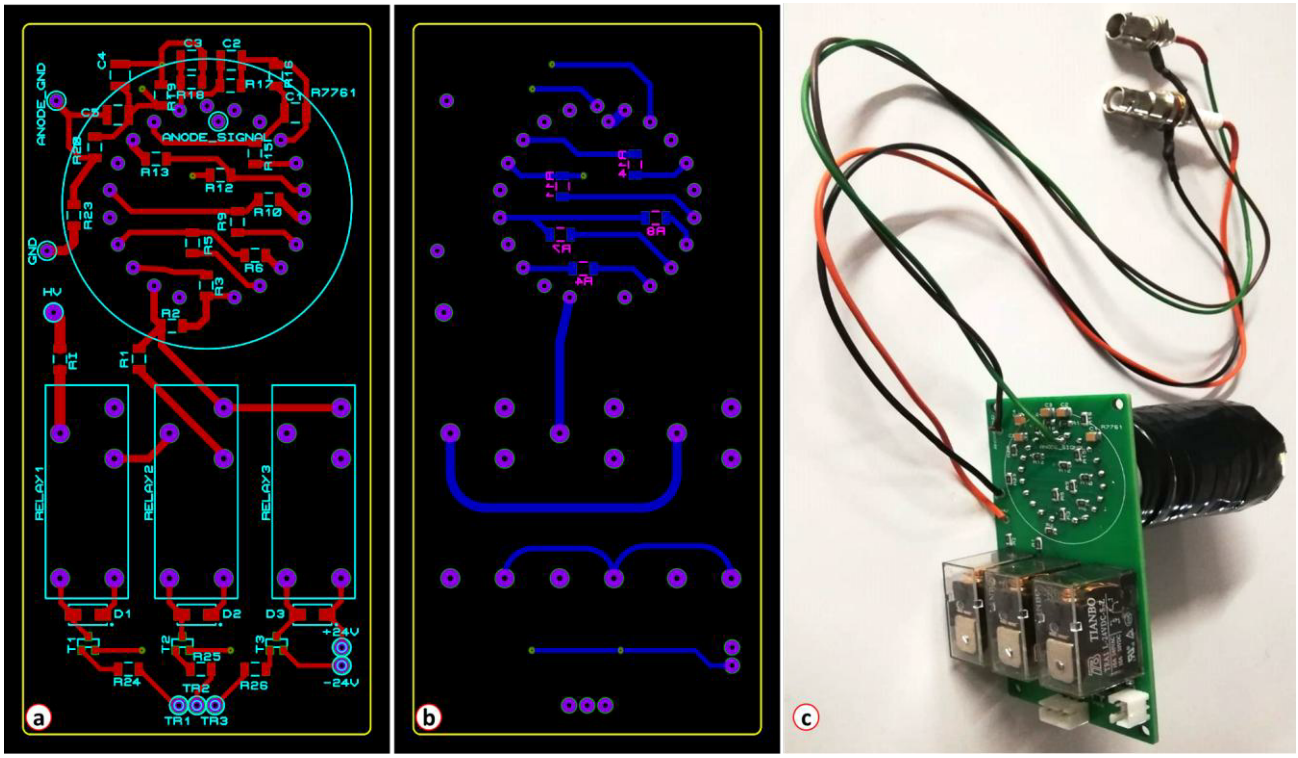

Figure 6. a) PCB layout view of the top side and b) bottom side c) Image of the electronic board with all soldering and assembly processes completed for the remote-controlled R7761 type PMT

The Arduino Uno board, a microcontroller that can be programmed to turn on and off the relays used to operate different modes on the remote-controlled card, was a key component of our system. The Arduino Uno board acts as the control

unit, executing the programmed instructions to switch the relays on and off. Arduino, coded in C++, was connected to the computer via serial communication. The graphical user interface (GUI) program for controlling the modes was written in C#. The screenshot of the main page and the modes are given in Figure 7.

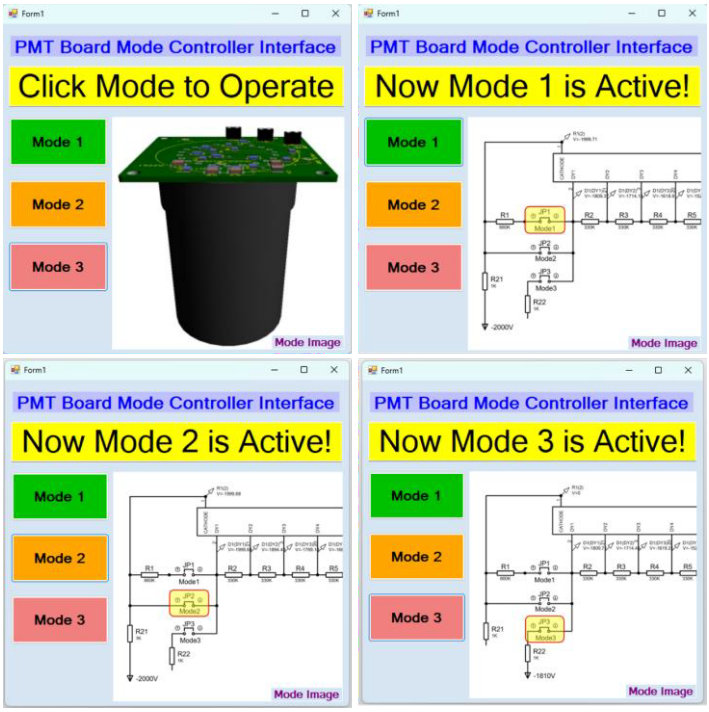

Figure 7. The screenshots of main (left top) and modes windows of the remote-controlled board's GUI.

3. Result and Discussion

Cosmic background radiation and a Co-60 (3.7 MBq) gamma radiation source were used in the same experiment to test all three SE module modes. We conducted the experiments at room temperature in a dark box in the lab and collected the experimental data using the same apparatus. Figure 8 displays the normalized waveform results for the gamma and cosmic radiation testing.

Modes 1 and 2 showed substantially larger signal sizes than Mode 3 for cosmic radiation. The signal amplitudes were about 70 mV for Mode 1, 65 mV for Mode 2, and 8 mV for Mode 3. Since there is no photocathode in the voltage-divider chain, there is a lot less space for cosmic radiation to interact. This makes the signal size 88% smaller in Mode 3 than it was in Mode 1. This proves that even at high voltages, Mode 3 is ineffective for detecting cosmic radiation.

As expected, Mode 2 exhibited a wider signal breadth than Mode 1 due to after-pulse contributions. Cosmological interactions with the photocathode material lead to the shorting of both the photocathode and the first dynode. Mode 3 showed a significantly smaller signal than Modes 1 and 2, which yielded similar signal sizes for gamma radiation. This suggests a clear variation in performance between the modes, highlighting the necessity of additional research to completely comprehend their applicability for various radiation detection circumstances.

We tested Mode 1 at three different voltage levels: 1800V, 2000V, and 2200V, to investigate performance variances. As anticipated, the signal size grew with higher applied voltages, as seen in Figure 9a (cosmic background) and Figure 9b (gamma radiation). Table 2 compiles these findings, demonstrating the SE module's versatility across a range of operating voltages and its capacity to detect gamma and cosmic radiation.

All things considered, the mode-specific traits and performance patterns highlight the SE module's potential as a technology for upcoming high-energy and radiation-resistant nuclear detectors.

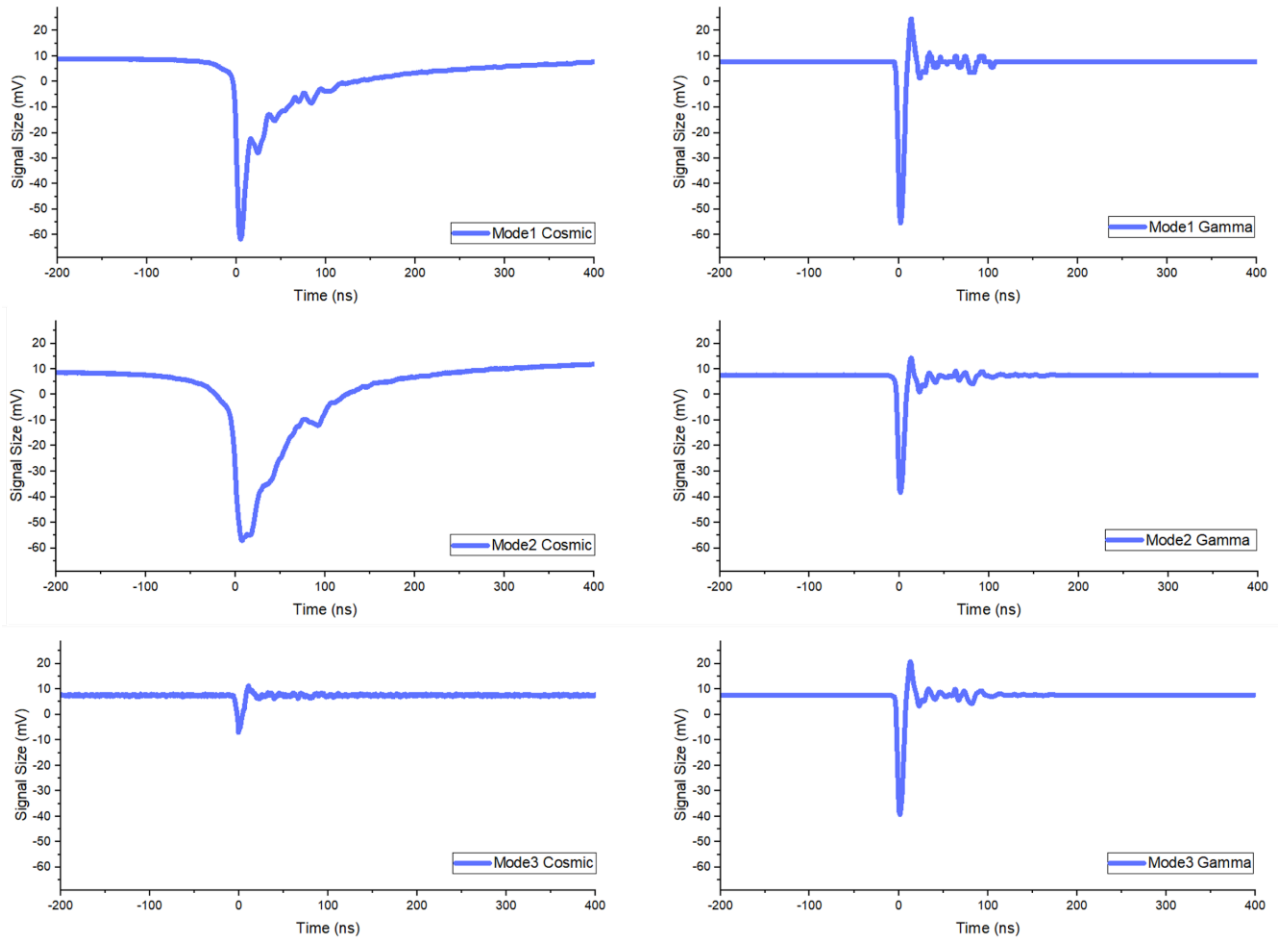

Figure 8. The normalized waveform results of all three modes for the cosmic and gamma radiation results.

The signal size received from the PMT varies according to the value of the applied voltage. The signal size increases within a specific operating voltage range as the applied voltage increases. Figure 9a shows the signal size of the cosmic background for 1800V, 2000V, and 2200V, while Figure 9b shows the signal size of Co-60 gamma radiation. These signal size variations are given in Table 2. The signal size of the PMT mode is increasing with the increasing voltage for both cosmic and gamma radiation, as expected. This study indicates that the SE module is a promising technology for future radiation-resistant nuclear and high-energy detectors.

Table 2. Approximate signal sizes (mV) of cosmic background and Co-60 gamma radiation for 1800V, 2000V, and 2200V voltages applied to the PMT.

	1800V	**2000V**	**2200V**
Cosmic Background	44.0	46.0	61.7
Co-60 Gamma	35.9	49.4	78.8

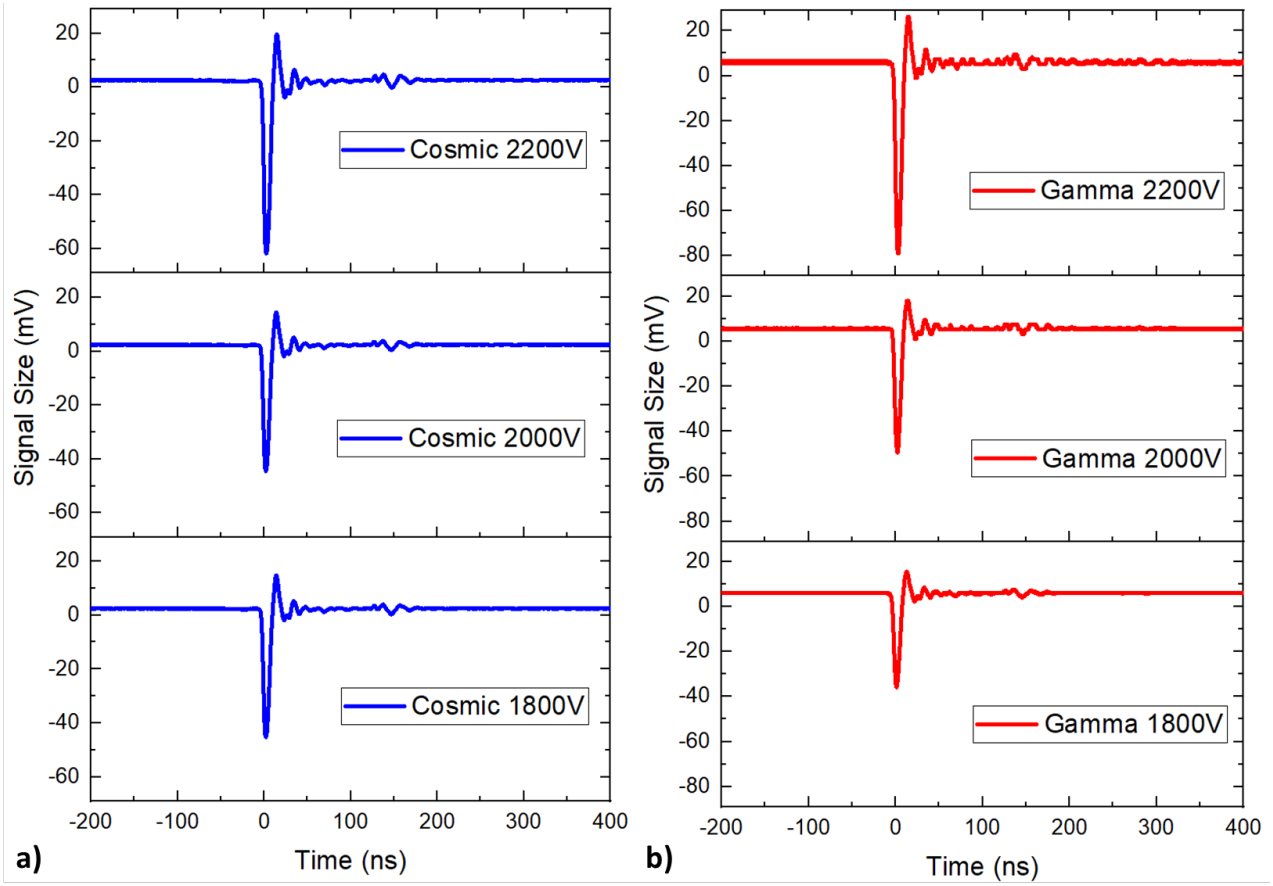

Figure 9. a) Pulse shapes of cosmic background radiation for 1800V, 2000V, and 2200V voltages applied to the PMT; **b)** Pulse shapes of Co-60 gamma radiation for 1800V, 2000V, and 2200V voltages applied to the PMT.

4. Conclusion

This study discusses the Hamamatsu R7761 PMT particle detector operating in three modes. We first provide information about the studies to solve the problems of particle detectors operating in high-radiation environments. Then, we explain one of these solutions, the SE Ionization Calorimeter. After explaining the SE calorimetry technique, we detail the design and fabrication of the electronic board for the operation of the R7761 photomultiplier detector. The results obtained by simulation highlight the differences between the design of manual and remote-controlled electronic boards. The electronic modules designed and produced for the study were then tested, and the results of the R7761 photomultiplier tube tests were obtained. We then describe the thorough preparation for the radiation testing process, which was essential to ensure the accuracy and reliability of our results. Finally, we present and explain the data obtained from our characterization tests with cosmic background and gamma radiation. All three SE module modes were tested with cosmic background radiation and a Co-60 gamma radiation source. Modes 1 and 2 exhibited substantially higher signal responses compared to Mode 3 in the detection of cosmic particles and gamma radiation. Mode 1 was further tested under three different voltages, revealing an increase in the signal size of the PMT mode with the increasing voltage for both cosmic and gamma radiation, as expected. This adaptability to different operating modes ensures the system's versatility and robustness, reassuring readers about its potential applications.

Acknowledgment

This work was supported by Scientific Research Projects (BAP) of Erciyes University, Türkiye, under the grant contracts of FBA-2022-12207, FBG-2022-11499, and FDS-2021-11525. Dr. Emrah Tiras is thankful for the support by the Turkish Academy of Sciences (TUBA) under the grant of the Outstanding Young Scientists Awards Program (GEBIP). We would like to thank the Office of the Dean for Research for providing the Lab's infrastructure at the ARGEPARK building at Erciyes University.

References

[1] V. Khachatryan, et. al., Dose rate effects in the radiation damage of the plastic scintillators of the CMS hadron endcap calorimeter, Journal of Instrumentation 11 (2016) T10004. https://doi.org/10.1088/1748-0221/11/10/T10004.

[2] U. Akgun, G. Funk, J. Corso, Z. Jia, D. Southwick, L. Adams, J. Kingyon, E. Tiras, T. Munhollon, E. Troendle, P. Bruecken, V. Khristenko, Y. Onel, Characterization of 1800 Hamamatsu R7600-M4 PMTs for CMS HF Calorimeter upgrade, Journal of Instrumentation 9 (2014) T06005.

[3] S. Liao, R. Erasmus, H. Jivan, C. Pelwan, G. Peters, E. Sideras-Haddad, A comparative study of the radiation hardness of plastic scintillators for the upgrade of the Tile Calorimeter of the ATLAS detector, J Phys Conf Ser 645 (2015) 012021. https://doi.org/10.1088/1742-6596/645/1/012021.

[4] A.M. Sirunyan, et. al, Measurements with silicon photomultipliers of dose-rate effects in the radiation damage of plastic scintillator tiles in the CMS hadron endcap calorimeter, JINST 15 (2020). https://doi.org/10.1088/1748-0221/15/06/p06009.

[5] J. Wetzel, E. Tiras, B. Bilki, Y. Onel, D. Winn, Using LEDs to stimulate the recovery of radiation damage to plastic scintillators, Nucl Instrum Methods Phys Res B 395 (2017) 13–16.

[6] J. Oliveira, V. Correia, E. Sowade, I. Etxebarria, R.D. Rodriguez, K.Y. Mitra, R.R. Baumann, S. Lanceros-Mendez, Indirect X-ray Detectors Based on Inkjet-Printed Photodetectors with a Screen-Printed Scintillator Layer, ACS Appl Mater Interfaces 10 (2018) 12904–12912. https://doi.org/10.1021/ACSAMI.8B00828/ASSET/IMAGES/LARGE/AM-2018-00828Q_0007.JPEG.

[7] W. Frass, R. Walczak, C4: Particle Physics Major Option Particle Detectors, (n.d.).

[8] P.W. Nicholson, Nuclear electronics, (1974).

[9] D.R. Winn, Y. Onel, Secondary Emission Calorimeter Sensor Development, J Phys Conf Ser 404 (2012) 012021.

[10] B. Bilki, K. Dilsiz, H. Ogul, Y. Onel, D. Southwick, E. Tiras, J. Wetzel, D.R. Winn, Secondary Emission Calorimetry, Instruments 6 (2022) 48. https://doi.org/10.3390/INSTRUMENTS6040048.

[11] R.G. Lye, A.J. Dekker, Theory of Secondary Emission, Physical Review 107 (1957) 977.

[12] B. Bilki, Secondary emission calorimetry R and D, 2014 IEEE Nuclear Science Symposium and Medical Imaging Conference, NSS/MIC 2014 (2016). https://doi.org/10.1109/NSSMIC.2014.7431155.

[13] A. Albayrak-Yetkin, B. Bilki, J. Corso, P. Debbins, G. Jennings, V. Khristenko, A. Mestvirisvilli, Y. Onel, I. Schmidt, C. Sanzeni, D. Southwick, D.R. Winn, T. Yetkin, Secondary Emission Calorimetry: Fast and Radiation-Hard, (2013).

[14] F. Ozok, T. Yetkin, E.A. Yetkin, E. Iren, M.N. Erduran, Geant4 simulation of a conceptual calorimeter based on secondary electron emission, Journal of Instrumentation 12 (2017) P07014. https://doi.org/10.1088/1748-0221/12/07/P07014.

[15] E. Tiras, Beam test results of Secondary Emission Ionization Calorimetry modules at Fermilab, Nucl Instrum Methods Phys Res A 1049 (2023) 168083. https://doi.org/10.1016/J.NIMA.2023.168083.

[16] E. Tiras, K. Dilsiz, H. Ogul, D. Southwick, B. Bilki, J. Wetzel, J. Nachtman, Y. Onel, D. Winn, Characterization of photomultiplier tubes in a novel operation mode for Secondary Emission Ionization Calorimetry, Journal of Instrumentation 11 (2016).

[17] G.A. Morton, Nuclear Radiation Detectors, Proceedings of the IRE 50 (1962).

[18] A. Artikov, J. Boudagov, D. Chokheli, G. Drake, M. Gallinaro, M. Giunta, J. Grudzinski, J. Huston, M. Iori, D. Kim, M. Kim, N. Kimura, S. Kuhlmann, S. Lami, R. Miller, K. Nakamura, L. Nodulman, A. Penzo, K. Sato, J. Suh, N. Turini, F. Ukegawa, Y. Yamada, CDF Central Preshower and Crack Detector Upgrade, (2007). https://arxiv.org/abs/0706.3922v1 (accessed April 4, 2024).

[19] H. Photonics, Photomultiplier Tubes: Basics and Application, 2006.